Restoration of Tissue Factor Pathway Inhibitor-2 in a Human Glioblastoma Cell Line Triggers Caspase-Mediated Pathway and Apoptosis

Joseph George,[1] Christopher S. Gondi,[1] Dzung H. Dinh,[2] Meena Gujrati,[3] and Jasti S. Rao[1,2]

Abstract

Purpose: The induction of apoptotic pathways in cancer cells offers a novel and potentially useful approach to improve patient responses to conventional chemotherapy. Tissue factor pathway inhibitor-2 (TFPI-2) is a protease inhibitor that is abundant in the extracellular matrix and highly expressed in noninvasive cells but absent or undetectable in highly invasive human glioblastoma cells.

Experimental Design: Using a recombinant adeno-associated viral vector carrying human TFPI-2 cDNA, we stably expressed TFPI-2 in U-251 cells, a highly invasive human glioblastoma cell line. Our previous studies showed that restoration of TFPI-2 in glioblastomas effectively prevents cell proliferation, angiogenesis, and tumor invasion. In this study, we determined whether TFPI-2 restoration could induce apoptosis through the caspase-mediated signaling pathway.

Results: The results from nuclear chromatin staining, terminal deoxynucleotidyl transferase–mediated dUTP nick end labeling assay, and fluorescence-activated cell sorting analysis showed increased apoptosis in U-251 cells after restoration of TFPI-2. Caspase-9 and caspase-3 activity assays showed increased activity, indicating enhanced apoptosis. Immunofluorescence for cleaved caspase-9 and caspase-3 depicted increased expression and colocalization of both molecules. Western blot analysis showed increased transcriptional activities of Fas ligand, tumor necrosis factor-α, Bax, Fas-associated death domain, and tumor necrosis factor receptor 1–associated death domain as well as elevated levels of cleaved caspases and poly(ADP-ribose) polymerase. Semiquantitative reverse transcription-PCR depicted increased expression of tumor necrosis factor-α and Fas ligand and the related death domains tumor necrosis factor receptor 1–associated death domain and Fas-associated death domain.

Conclusions: Taken together, these results show that restoration of TFPI-2 activates both intrinsic and extrinsic caspase-mediated, proapoptotic signaling pathways and induces apoptosis in U-251 cells. Furthermore, our study suggests that recombinant adeno-associated viral vector–mediated gene expression offers a novel tool for cancer gene therapy.

Glioblastomas are highly invasive and aggressive primary brain tumors associated with a dismal prognosis (1). Glioblastomas comprise 23% of primary brain tumors in the United States and are the most commonly diagnosed brain tumor in adults (2). The median survival of patients with glioblastoma treated with surgery, radiotherapy, and chemotherapy is from 10 to 22 months (3). Although the understanding of the pathophysiology of gliomas has increased significantly over the past few years, an effective treatment has not been developed for this type of cancer. Limits in the efficacy of current treatment modalities call for the development of novel therapeutic approaches targeting the specific biological features of glioblastomas.

Human tissue factor pathway inhibitor-2 (TFPI-2) is a Kunitz-type proteinase inhibitor that acts against a wide range of serine proteases through their nonproductive interaction with a P_1 residue in its first Kunitz-type domain (4). A wide variety of cells, including keratinocytes (5), dermal fibroblasts (5), smooth muscle cells (6), synoviocytes (7), and endothelial cells (8), synthesize and secrete TFPI-2 primarily into the extracellular matrix (ECM). Three isoforms of TFPI-2 are synthesized by these cells and migrate with an apparent molecular weight of 33, 31, and 27 kDa due to differential glycosylation (9). TFPI-2 exhibits strong inhibitory activity toward a broad spectrum of proteinases, including trypsin, plasmin, chymotrypsin, cathepsin G, plasma kallikrein, and the factor VIIa-tissue factor complex. In contrast, TFPI-2 exhibits little or no inhibitory activity toward urokinase-type plasminogen activator, tissue-type

Authors' Affiliations: Departments of [1]Cancer Biology and Pharmacology, [2]Neurosurgery, and [3]Pathology, University of Illinois, College of Medicine at Peoria, Peoria, Illinois

Received 12/20/06; revised 2/28/07; accepted 3/6/07.

Grant support: National Cancer Institute grants CA 75557, CA 92393, CA 95058, and CA 116708; National Institute of Neurological Disorders and Stroke grants NS47699 and NS5729; Caterpillar, Inc.; and OSF Saint Francis, Inc., Peoria, IL (J.S. Rao).

The costs of publication of this article were defrayed in part by the payment of page charges. This article must therefore be hereby marked *advertisement* in accordance with 18 U.S.C. Section 1734 solely to indicate this fact.

Requests for reprints: Jasti S. Rao, Department of Cancer Biology and Pharmacology, University of Illinois, College of Medicine at Peoria, Peoria, IL 61605. Phone: 309-671-3445; Fax: 309-671-3442; E-mail: jsrao@uic.edu.

doi:10.1158/1078-0432.CCR-06-3023

plasminogen activator, and α-thrombin (10). Recent studies have shown that TFPI-2 expression plays a significant role in inhibiting tumor invasion and metastasis by a mechanism that involves its inhibitory activity (11–13). However, little is known about the role of TFPI-2 in the induction of apoptotic pathways in glioblastomas.

Apoptosis, the programmed cell death, is critical for the development and maintenance of healthy tissues. There are two alternative pathways that initiate apoptosis: one is mediated by death receptors on the cell surface and the other is mediated by mitochondria (14, 15). Fas ligand (FasL) and tumor necrosis factor (TNF)-α play important roles by rapidly inducing apoptosis under numerous physiologic and pathologic conditions (16). On ligand activation to their receptors, Fas and TNF receptor (TNFR) 1 associate with death domain containing adaptor proteins Fas-associated death domain (FADD) and TNFR1-associated death domain (TRADD), which contain a death domain homologous region (17, 18). FADD has a COOH-terminal death domain interacting with the cytoplasmic tail of the membrane receptor and an NH_2-terminal death effector domain interacting with the caspase-8 (19). Clustering of the receptors on stimulation causes FADD to oligomerize caspase-8 and triggers a caspase-mediated signaling pathway. Caspase-8 subsequently activates downstream effector caspases, such as caspase-3, resulting in the cleavage of proteins involved in the execution of apoptosis. Alternatively, apoptosis driven by TNFR1 binding to TRADD involves association of TRADD and FADD, which then leads to activation of caspase-8 (20). Further, overexpression of TRADD leads to nuclear factor-κB activation and apoptosis in the absence of TNFR1 (21).

Proapoptotic stimuli, such as DNA damage and oxidative stress, require a mitochondrial-dependent step that involves the release of cytochrome *c*, which is normally located in the intermembrane space (22, 23). Liberated cytochrome *c* then initiates formation of an apoptosome along with apoptotic protease-activating factor-1 in the presence of adenosine nucleotides (22, 24). The apoptosome processes procaspase-9 into a large active fragment and a small fragment by self-cleavage at Asp^{315} and then initiates a sequential pathway that ends with DNA fragmentation and eventual apoptosis (25–27). In contrast, apoptosis-inducing factor translocates from mitochondria via the cytoplasm to the nucleus where it interacts with DNA and causes nuclear condensation and DNA fragmentation (23). Thus, the mitochondrial apoptotic pathway involves both caspase-dependent and caspase-independent processes in apoptotic cell death. The pathophysiologic roles of the apoptotic signaling pathway have recently been identified in several human tumors, including glioblastomas (28–31). In the present investigation, we selected an established glioblastoma cell line, U-251, where TFPI-2 expression is totally absent due to the aberrant hypermethylation of TFPI-2 promoter CpG islands. We restored TFPI-2 protein levels in U-251 cells through an adeno-associated viral vector carrying *TFPI-2* gene and evaluated the effect of restored TFPI-2 on the signaling of cell surface death receptors as well as mitochondrial-mediated proapoptotic pathways.

Materials and Methods

Cloning of human TFPI-2 cDNA

The procedures for the cloning and purification of the recombinant adeno-associated viral vector carrying human TFPI-2 cDNA (rAAV-TFPI-2) used in the present study have been described previously (13). Briefly, the entire coding region (a 0.8-kb fragment) of the human *TFPI-2* gene was cloned into the adeno-associated viral vector (pCMV-MCS) at the *Bam*H1 site. The plasmids were propagated in JM109-competent (Promega Corp.) *Escherichia coli* strain. The viral vector particles were propagated in the AAV-293 cell line (Stratagene), which produces higher viral titers. The viral preparation was purified by ultracentrifugation using an iodixanol density gradient system.

Cell culture conditions

The highly invasive human glioblastoma cell line U-251 was procured from the National Cancer Institute. The cells were propagated in RPMI 1640 (Mediatech) supplemented with 10% fetal bovine serum in a humidified atmosphere containing 5% CO_2 at 37°C. rAAV-TFPI-2 was suitably diluted in serum-free medium at concentrations of 25, 50, and 100 multiplicities of infection (MOI). The virus particles were reconstituted in a minimum volume of serum-free medium and added to the cell monolayers. Cells were then incubated at 37°C for 1 to 2 h to complete the transduction of virus particles into the cells. The serum-free medium was replaced with serum-containing medium and cells were incubated for desired times.

Western blot analysis for TFPI-2

ECM proteins were extracted from U-251 parental cells—cells transfected with an empty viral vector or with 25, 50, and 100 MOI of rAAV-TFPI-2. ECM proteins were also extracted from Hs 683 cells, a low-grade, noninvasive astrocytoma (procured from the American Type Culture Collection); the Hs 683 cells were used as a standard for TFPI-2, as these cells highly express TFPI-2. All the cell cultures were treated with 200 nmol of phorbol 12-myristate 13-acetate (Cell Signaling Technology) per milliliter of the culture medium overnight. The cultures were washed with PBS thrice and then lysed with PBS containing 0.5% Triton X-100 (v/v) for 20 min at room temperature. After aspirating the Triton X-100 along with the lysed cells, the remaining ECM was washed thrice with PBS and then twice with 20 mmol/L Tris-HCl (pH 7.4) containing 100 mmol/L NaCl and 0.1% (v/v) Tween 20. The culture dishes were then examined under a light microscope and ensured that no visible cells were present in the dishes. To collect ECM proteins, 200 μL of 1× SDS-PAGE sample buffer were added to each dish and agitated for 20 min at room temperature. About 30 μL of these extracts were resolved on 12% SDS-PAGE and the proteins were subsequently transferred to a nitrocellulose membrane (Bio-Rad Laboratories). The membranes were blocked with 10% nonfat dry milk and incubated overnight at 4°C with anti-TFPI-2 antibody diluted at 1:3,000 (kindly provided by Dr. Walter Kisiel, University of New Mexico, Albuquerque, NM). After three washes, the membranes were incubated with a 1:5,000 diluted peroxidase-conjugated secondary antibody (Biomeda). TFPI-2 proteins were developed using an enhanced chemiluminescence method according to the manufacturer's instructions (Amersham Biosciences). The Western blots were quantified using Image-Pro Discovery software (Media Cybernetics) to evaluate the percentage restoration of TFPI-2 protein levels in U-251 cells.

Nuclear chromatin staining for apoptosis

Double nuclear staining was carried out to study the induction of apoptosis in U-251 cells after restoration of TFPI-2. U-251 parental cells were cultured on 12-well culture dishes at a density of 2×10^4 per well. After 24 h, the cells were transfected with rAAV-TFPI-2 at concentrations of 25, 50, and 100 MOI in serum-free medium for 2 h. We used an empty vector transfected at 100 MOI for the vector control. The serum-free medium was replaced with serum-containing medium and the cultures were incubated for 48 h. The cells were removed from the incubator and 2 μL (2 μg) of Hoechst 33342 (Invitrogen) were added per milliliter of culture medium. The cells were mixed gently and incubated for 15 min. Afterwards, 10 μL (concentration, 100 mg/mL) of membrane-impermeable propidium iodide (Calbiochem, EMD

Biosciences) were added per milliliter of culture medium, mixed gently, and allowed to stand for 1 min. The cells were then observed under a fluorescent microscope (Olympus BX61) using the RGB filter and photographed.

Terminal deoxynucleotidyl transferase–mediated dUTP nick end labeling assay

The terminal deoxynucleotidyl transferase–mediated dUTP nick end labeling (TUNEL) assay was done to detect apoptotic cells after transfection with rAAV-TFPI-2. U-251 parental cells were cultured on eight-well chamber slides at a density of 2×10^3 per well. Twenty-four hours later, the cells were transfected with rAAV-TFPI-2 at concentrations of 50 and 100 MOI in serum-free medium. We used an empty vector transfected at 100 MOI for the vector control. The cultures were terminated at 48 h after transfection, and the cells were fixed in 10% phosphate-buffered formalin for 15 min. TUNEL staining for detection of apoptotic cells was done using the TUNEL Apoptotic Detection kit (Upstate Cell Signaling Solutions) as per the manufacturer's instructions. Briefly, the fixed cells were washed in PBS thrice (5 min/wash). The cells were then incubated with 0.05% Tween 20 in PBS containing 0.2% bovine serum albumin for 15 min at room temperature. The cells were washed twice in PBS and incubated with 50 μL of terminal deoxynucleotidyl transferase end-labeling cocktail for 60 min at room temperature. The reaction was terminated, and slides were washed thrice in PBS and blocked with blocking buffer for 20 min at room temperature. Then, the slides were incubated with 50 μL of avidin-FITC in the dark for 30 min at room temperature, washed thrice in PBS, and mounted with antifading gel mount (Biomeda). Slides were allowed to dry in the dark, observed under a fluorescent microscope (Olympus BX61), and photographed. Fluorescent apoptotic cells were quantitatively evaluated (10 randomly selected microscopic fields per sample) using Image-Pro Plus software (Media Cybernetics).

Fluorescence-activated cell sorting analysis

Fluorescence-activated cell sorting (FACS) based on DNA fragmentation was done to determine the percentage of apoptotic cells after TFPI-2 restoration. U-251 parental cells were cultured on six-well plates (Corning Life Sciences) at a density of 1×10^5 per well. After 24 h, the cells were transfected with rAAV-TFPI-2 at concentrations of 50 and 100 MOI in serum-free medium. An empty viral vector transfected at a concentration of 100 MOI was used as a vector control. The cells were harvested at 48 h after transfection using TrypLE Express (Invitrogen) and washed once with PBS. The cells were then dispersed in 1 mL of membrane-permeable propidium iodide (50 μg/mL; BioSure) and incubated for 20 to 30 min in the dark at 4°C. The cells were sorted on a FACS machine (FACSCalibur, Becton Dickinson), and the DNA content was analyzed based on the red fluorescence of propidium iodide at 488 nm. Data are represented in a dot plot graph and FACS histogram.

Fluorometric protease activity assay

Protease activity assay was carried out to measure the increased enzymatic activity of caspase-9 after TFPI-2 restoration in U-251 cells. The assay is based on detection of cleavage of the fluorescent-tagged peptide Leu-Glu-His-Asp-7-amino-4-trifluoromethylcoumarin by caspase-9. U-251 parental cells were cultured in 100-mm plates (Corning Life Sciences) at a density of 1×10^6 per plate. After 24 h, the cells were transfected with rAAV-TFPI-2 at concentrations of 50 and 100 MOI in serum-free medium. A simultaneous transfection was carried out with an empty viral vector at a concentration of 100 MOI to use as a vector control. The cells were harvested at 48 h after transfection and counted. The caspase-9 activity assay was done using a fluorometric protease activity assay kit (BioVision Research Products) as per the manufacturer's instructions. Briefly, approximately 2×10^6 cells were suspended in chilled lysis buffer and incubated with 5 μL of 1 mmol/L Leu-Glu-His-Asp-7-amino-4-trifluoromethylcoumarin and incubated at 37°C for 2 h. The final fluorescent product was measured on a fluorometer (Fluoroskan Ascent FL, Thermo Labsystems) with a 390 nm excitation filter and 510 nm emission filter. The assay was carried out in four independent samples in duplicate, and the data were quantitatively represented as percentage activity of caspase-9.

Activity assay for caspase-3

The activity assay for caspase-3 (colorimetric) was done using a kit (Sigma) as per the manufacturer's instructions. The cells were cultured and transfected with rAAV-TFPI-2 as described above. The harvested cells were transferred to 96-well plates and treated with the caspase-3 peptide substrate conjugated with *p*-nitroaniline (Ac-DEVD-pNA), and the release of the *p*-nitroaniline by caspase-3 was measured on a microplate reader at 405 nm. The assay was carried out in four independent samples in triplicate. Data are quantitatively represented as percentage activity of caspase-3.

Double immunofluorescent staining

U-251 parental cells were cultured on eight-well chamber slides at a density of 2×10^3 per well. After 24 h, the cells were transfected with rAAV-TFPI-2 at concentrations of 50 and 100 MOI in serum-free medium. We used an empty viral vector transfected at a concentration of 100 MOI for the vector control. The cultures were terminated at 48 h after transfection, and cells were fixed in cold acetone for 10 min. Cells were then washed twice in PBS and blocked with 1% bovine serum albumin in PBS for 30 min. The cells were then treated with 1:50 diluted (1% bovine serum albumin in PBS) goat polyclonal human-specific cleaved caspase-9 (Santa Cruz Biotechnology) and 1:200 diluted rabbit monoclonal anti-human cleaved caspase-3 (Cell Signaling Technology) primary antibodies simultaneously and incubated overnight at 4°C. The cells were then washed thrice in PBS and incubated with Texas red–conjugated anti-goat (Biomeda) and FITC-conjugated anti-rabbit (Biomeda) secondary antibodies at room temperature for 1 h. The cells were further washed and treated with 1:100 diluted Hoechst 33342 for 5 min at room temperature for nuclear counterstaining. Cells were mounted with antifading gel mount and examined under a fluorescent microscope (Olympus BX61) using both dsRed and green fluorescent protein filters for the expression of cleaved caspase-9 and cleaved caspase-3, respectively. The pictures were then merged electronically with Hoechst 33342 staining using Spot Advanced software (Meyer Instruments).

Western blot analysis for molecules involved in the caspase-mediated apoptotic pathway

Preparation of cell lysate. U-251 parental cells were cultured in 100-mm plates at a density of 1×10^6 per plate. After 24 h, the cells were transfected with rAAV-TFPI-2 at concentrations of 50 and 100 MOI in serum-free medium as described above. An empty vector was transfected at a concentration of 100 MOI and used as a vector control. All the cultures were terminated after 48 h. The cells were washed twice with ice-cold PBS and scraped with 1 mL PBS. Cells were centrifuged at 12,000 rpm for 10 min at 4°C in an Eppendorf centrifuge. The supernatant was discarded and the cell pellet was suspended in freshly prepared radioimmunoprecipitation assay buffer with protease inhibitors [50 mmol/L Tris-HCl (pH 7.4) containing 1% NP40, 150 mmol/L NaCl, 1 mmol/L activated sodium orthovanadate, 1 mmol/L sodium fluoride, 1 mmol/L phenylmethylsulfonyl fluoride, 1 mmol/L EDTA, 5 μg/mL aprotinin, and 5 μg/mL pepstatin] and sonicated gently in an ultracell disruptor (Sonic Dismembrator, Fisher Scientific). Cells were centrifuged at 14,000 rpm for 10 min at 4°C and the supernatants were collected. The protein concentration in the supernatant was determined using bicinchoninic acid (Pierce Biotechnology) protein assay as described by Smith et al. (32). The samples were stored at -20°C until assayed. To measure released cytochrome *c* levels, mitochondria were isolated from the total cell lysate using the mitochondria isolation kit for cultured cells (Pierce Biotechnology) and the cytosol fraction was used to determine cytochrome *c* levels.

Western blot analysis. Protein concentrations ranging from 5 to 100 μg were used for analysis of various molecules involved in the caspase-mediated apoptotic pathway after prior standardization of each molecule. The protein samples were mixed with 6× loading buffer containing 600 mmol/L DTT. The samples were kept in a boiling water bath for 3 min and instantly loaded on SDS-polyacrylamide gel ranging from 7% to 12% depending on the molecular weight of the protein. The separated proteins were electrophoretically transferred to a nitrocellulose membrane. The membranes were treated with 10% nonfat dry milk for 30 min at room temperature to block the nonspecific sites. The membranes were then incubated overnight at 4°C with either polyclonal or monoclonal human-specific antibodies for various protein molecules. All antibodies were diluted at either 1:1,000 or per manufacturer's instructions in 5% nonfat dry milk. The antibodies for caspase-9, caspase-8, caspase-7, caspase-6, caspase-3, lamin A, Bcl-2, apoptotic protease-activating factor-1, Bax, and FasL were purchased from Cell Signaling Technology; antibodies for TRADD and FADD were purchased from Santa Cruz Biotechnology; antibodies for caspase-10 and TNF-α were purchased from Abcam; the DFF40 antibody was purchased from Chemicon International; the poly(ADP-ribose) polymerase (PARP) antibody was purchased from Oncogene-Calbiochem (EMD Biosciences); and the cytochrome *c* antibody was from BD PharMingen. After an overnight incubation, the membranes were washed thrice in 0.05% Tween 20 and treated with 1:2,000 diluted anti-rabbit or anti-mouse horseradish peroxidase–conjugated secondary antibodies (Biomeda) at room temperature for 1 h. The membranes were then washed thrice in 0.05% Tween 20 and treated with enhanced chemiluminescence reagent. Finally, the membranes were exposed to autoradiography hyperfilm (Amersham Biosciences). The thickness of the band on the film was adjusted appropriately with different exposure times. The membranes were reprobed using Western reprobe buffer (GBiosciences) and analyzed for glyceraldehyde-3-phosphate dehydrogenase (GAPDH) content to show that similar amounts of protein were loaded in each lane. Mouse monoclonal GAPDH antibody (Novus Biologicals) was used.

Semiquantitative reverse transcription-PCR

U-251 parental cells were cultured in six-well chambers (Corning Life Sciences) up to 80% confluence and transfected with rAAV-TFPI-2 at concentrations of 50 and 100 MOI. We used an empty viral vector transfected at a concentration of 100 MOI for the vector control. Total cellular RNA was isolated using RNeasy kit (Qiagen) according to the manufacturer's instructions. Gene-specific primers were designed using Beacon Designer software (Premier Biosoft International). We used the following primer sequences: TNF-α, 5′-CACCACGCTCTTCTGCCTGCTG-3′ (forward) and 5′ TCTGGTAGGAGACGGCGATGCG-3′ (reverse); FasL, 5′-AGCAAATAGGCCACCCCAGTCC-3′ (forward) and 5′-TGGCTCAGGGGCAGGTTGTTG-3′ (reverse); TRADD, 5′-CGCTCTGTGGGTCTCAAATGGC-3′ (forward) and 5′-AGTCCTCTGCCAGGCTGGTGAG-3′ (reverse); FADD, 5′-TTGGAGAAGGCTGGCTCGTCAG-3′ (forward) and 5′-ACATGGCCCCACTCCTGTTCTG-3′ (reverse); and GAPDH, 5′-AAGGCTGTGGGCAAGGTCATCC-3′ (forward) and 5′-GGAGGAGTGGGTGTCGCTGTTG-3′ (reverse). All the primers were transcribed with ~100 ng of isolated total RNA using a one-step reverse transcription-PCR (RT-PCR) kit (Invitrogen) in a thermocycler (GeneAmp PCR Systems 9700, Applied Biosystems) under the following reaction conditions: cDNA synthesis, 50°C for 30 min; inactivation, 94°C for 2 min; PCR amplification of 35 cycles, denature at 94°C for 20 s, annealing at 58°C for 30 s, chain extension at 72°C for 45 s, and a final chain extension at 72°C for 10 min. The amplified products were separated on 1% agarose gels with ethidium bromide and visualized using a transilluminating UV (Alpha Innotech Corp.). *GAPDH* was used as a housekeeping gene.

We used the same primer sequences for quantitative real-time RT-PCR analysis of TNF-α, FasL, TRADD, and FADD mRNA expression. Real-time RT-PCR was carried out using a one step RT-PCR kit with SYBR Green (Bio-Rad Laboratories) on a real-time PCR machine (iCycler, Bio-Rad Laboratories) under the following reaction conditions: cDNA synthesis at 10 min at 50°C, reverse transcriptase inactivation at 95°C for 5 min, thermal cycling and detection (up to 35 cycles) at 95°C for 10 s, and data collection at 56°C for 30 s. Approximately 100 ng of total isolated RNA were transcribed. *GAPDH* was used as a housekeeping gene.

Statistical analysis

Arithmetic mean and SD were calculated for all quantitative data. The results were statistically evaluated using one-way ANOVA. Mean control values were compared with empty vector and rAAV-TFPI-2–treated cultures at 50 and 100 MOI using least significant difference method. A P value of <0.05 was considered as statistically significant.

Results

Restoration of TFPI-2 in U-251 cells. Previous studies from our laboratory have shown that TFPI-2 plays an important role in the regulation of cell migration, invasion, and angiogenesis (12, 13). The results of the present study proved that TFPI-2 restoration in U-251 cells triggers caspase-mediated signaling pathway and apoptosis. Western blot analysis (Fig. 1) shows that U-251 cells transfected with rAAV-TFPI-2 successfully restored TFPI-2 protein levels in U-251 cells in a dose-dependent manner. The three characteristic bands of TFPI-2 at 33, 31, and 27 kDa were distinctly present in the protein extracts of the U-251 cells transfected with rAAV-TFPI-2. In contrast, TFPI-2 protein was completely absent in U-251 parental cells and cells transfected with the empty vector. Figure 1B shows the percentage restoration of TFPI-2 expression in U-251 cells when correlated with TFPI-2 expression in the nonmalignant tumor cell line Hs 683.

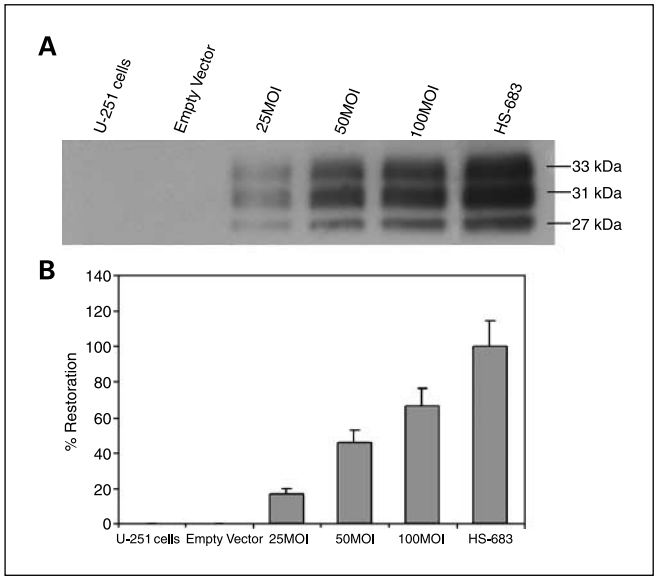

Fig. 1. *A,* Western blot analysis for the expression of TFPI-2 in the ECM of U-251 glioblastoma cells. U-251 cells were transfected with rAAVs engineered to express human TFPI-2 at concentrations of 25, 50, and 100 MOI, and the levels of TFPI-2 in the ECM of U-251 cells were determined by Western blotting. A 0.8-kb fragment of human TFPI-2 was cloned into a human adeno-associated viral vector (pCMV-MCS) at the *Bam*H1 site. TFPI-2 protein from the ECM extracts of Hs 683 cells was used as a positive control. *B,* quantitative evaluation of the percentage restoration of TFPI-2 protein levels in U-251 cells. The Western blots were quantified using Image-Pro Discovery software to assess the percentage restoration of TFPI-2 protein levels in U-251 cells. Columns, mean ($n = 6$); bars, SD.

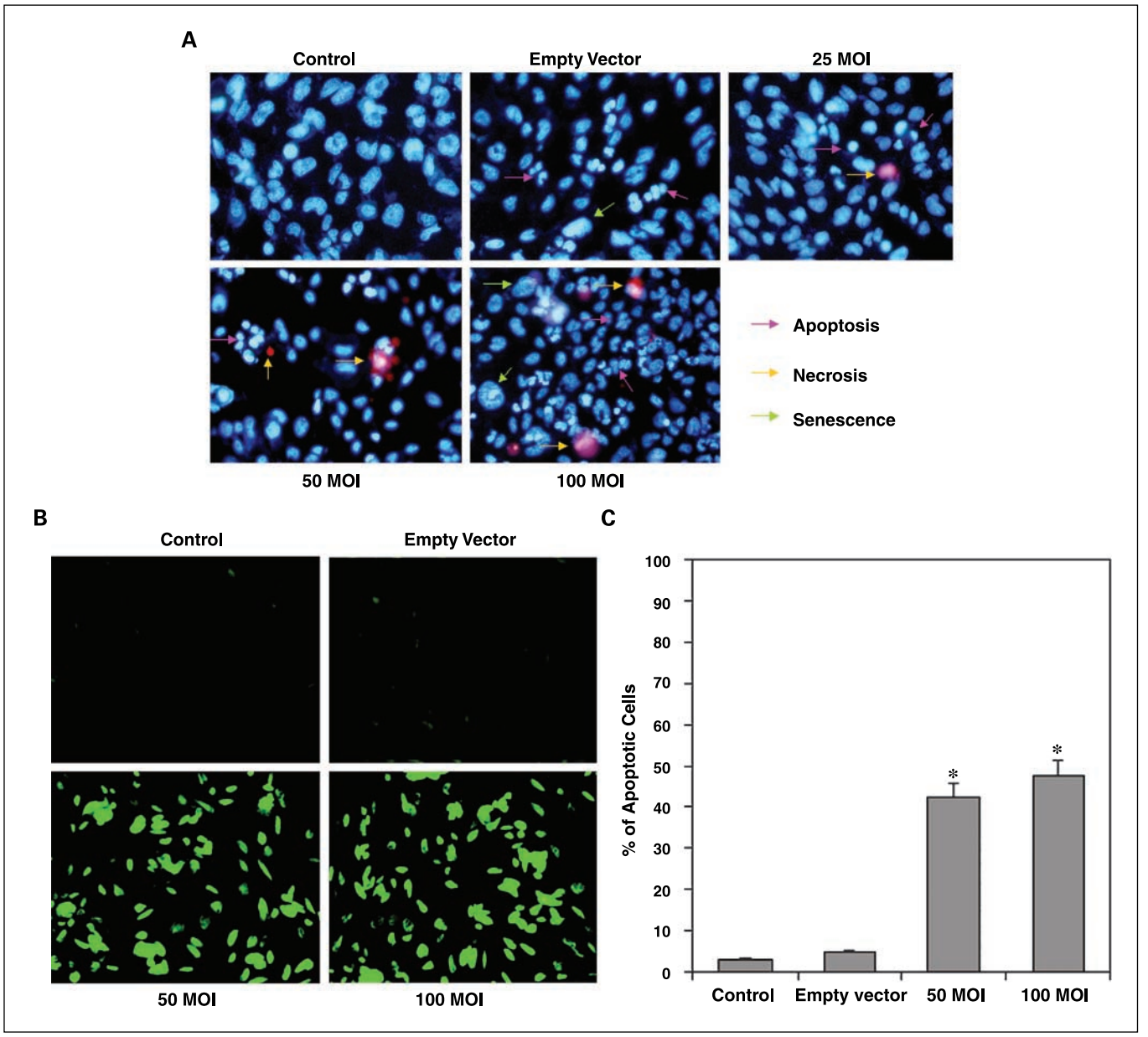

Fig. 2. *A,* nuclear chromatin staining of U-251 cells with Hoechst 33342 (bis-benzimidazole) and membrane-impermeable propidium iodide. U-251 cells were transfected with rAAV-TFPI-2 at concentrations of 25, 50, and 100 MOI in serum-free medium. An empty vector transfected at a concentration of 100 MOI was used as a vector control. *B,* fluorescent TUNEL assay of rAAV-TFPI-2 – transfected U-251 cells. Cells were transfected with 50 and 100 MOI of rAAV-TFPI-2 in serum-free medium. An empty vector transfected at 100 MOI was used as a vector control. *C,* quantitative evaluation of TUNEL assay. We used Image-Pro Discovery software to quantify the results of the TUNEL assay. Data are representative of four independent experiments done in duplicate. *, $P < 0.001$.

Increased apoptosis in nuclear chromatin staining. We examined the rate of apoptosis, necrosis, and senescence in U-251 cells after restoration of TFPI-2 using a double nuclear staining technique using Hoechst 33342 (bis-benzimidazole) and membrane-impermeable propidium iodide. Hoechst 33342 is capable of penetrating the nuclear membrane and stains the chromatin blue, thereby allowing for the visual differentiation of the apoptotic nuclei. In contrast, membrane-impermeable propidium iodide is unable to penetrate the cells undergoing apoptosis and can stain only the necrotic cells. The results of double nuclear staining are shown in Fig. 2A. As evident from the figure, the staining indicates a dose-dependent increase of apoptosis and necrosis as well as senescent cells at 48 h after TFPI-2 restoration. We observed a marked increase in the number of apoptotic cells (where the nuclei are shrunk and stained in a zigzag manner) at 100 MOI.

Increased apoptosis as indicated by TUNEL assay after TFPI-2 restoration. To confirm the apoptosis observed in the results from the nuclear chromatin staining, we next did the TUNEL assay, which is a highly specific technique that shows the apoptotic cells both in cell cultures and paraffin sections. The TUNEL assay indicated a large number of apoptotic cells in the U-251 cell cultures transfected with rAAV-TFPI-2 both at 50 and 100 MOI (Fig. 2B). However, staining was almost absent or insignificant in both U-251 parental cells and cells transfected with the empty vector. Quantitative evaluation of

the TUNEL assays using computer-assisted Image-Pro Plus software revealed 43% and 48% apoptotic cells after treatment with rAAV-TFPI-2 at 50 and 100 MOI, respectively (Fig. 2C).

Increased apoptosis as indicated by flow cytometry and DNA fragmentation analyses. Flow cytometry is an excellent tool for accurate detection of apoptotic cells. We did flow cytometry for DNA fragmentation in U-251 cells after TFPI-2 restoration via transfection of rAAV-TFPI-2. Figure 3A represents the dot plot of U-251 cells after transfection with rAAV-TFPI-2 at 50 and 100 MOI. A marked increase in cell population was observed in the column R1 area, which represents apoptotic cells. However, there was no significant difference in the cell population in the column R1 area between U-251 parental cells and cells transfected with the empty vector. Figure 3B denotes the FACS histogram of DNA fragmentation analysis after restoration of TFPI-2 in U-251 cells. As indicated in the figure, the R1 area represents the apoptotic cell population. It is clearly evident that the apoptotic cell population is remarkably increased after transfection of U-251 cells with rAAV-TFPI-2. The data also show a strong positive correlation with the results of the fluorescent TUNEL assay for the detection of apoptotic cells. Figure 3C represents the quantitative evaluation of FACS data for DNA fragmentation analysis using Image-Pro Plus software. Quantitative analysis showed 41% and 46% apoptotic cells after treatment with rAAV-TFPI-2 at 50 and 100 MOI, respectively.

TFPI-2 restoration enhances activity of caspase-9 and caspase-3. We have measured the activity of mature caspase-9 using a specific and sensitive fluorometric assay after TFPI-2 restoration in U-251 cells. Figure 4A shows caspase-9 activity in U-251 parental cells—cells transfected with the empty vector or rAAV-TFPI-2 at 50 and 100 MOI. A significant increase ($P < 0.001$) was observed in the activity of mature caspase-9 after transfection of U-251 parental cells with rAAV-TFPI-2 at both 50 and 100 MOI. The increase was >2.5-fold at 100 MOI when compared with the caspase-9 activity in U-251 parental cells. We did not detect a significant difference in the activity of caspase-9 between U-251 parental cells and cells transfected with the empty vector.

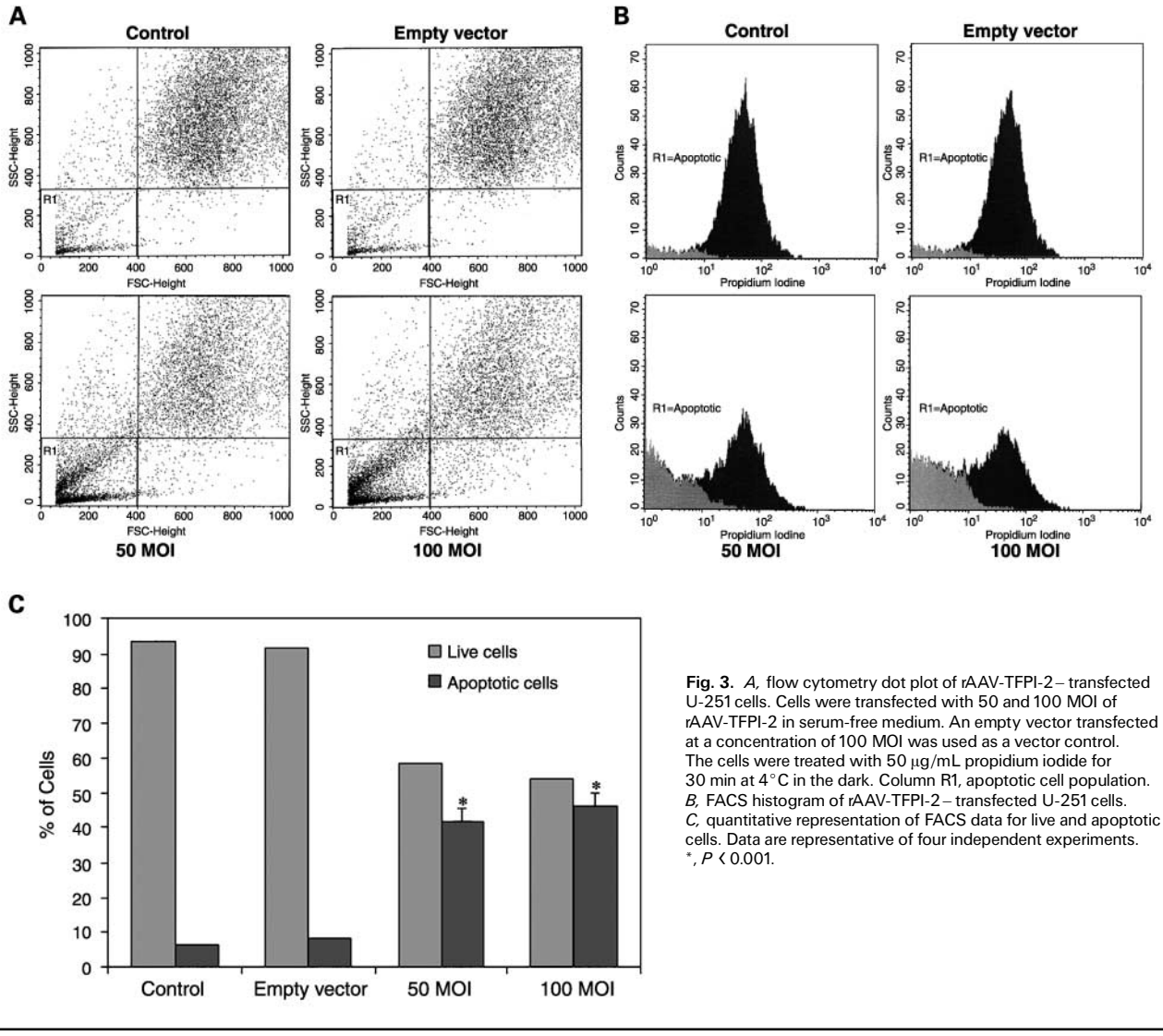

Fig. 3. *A,* flow cytometry dot plot of rAAV-TFPI-2–transfected U-251 cells. Cells were transfected with 50 and 100 MOI of rAAV-TFPI-2 in serum-free medium. An empty vector transfected at a concentration of 100 MOI was used as a vector control. The cells were treated with 50 μg/mL propidium iodide for 30 min at 4°C in the dark. Column R1, apoptotic cell population. *B,* FACS histogram of rAAV-TFPI-2–transfected U-251 cells. *C,* quantitative representation of FACS data for live and apoptotic cells. Data are representative of four independent experiments. *, $P < 0.001$.

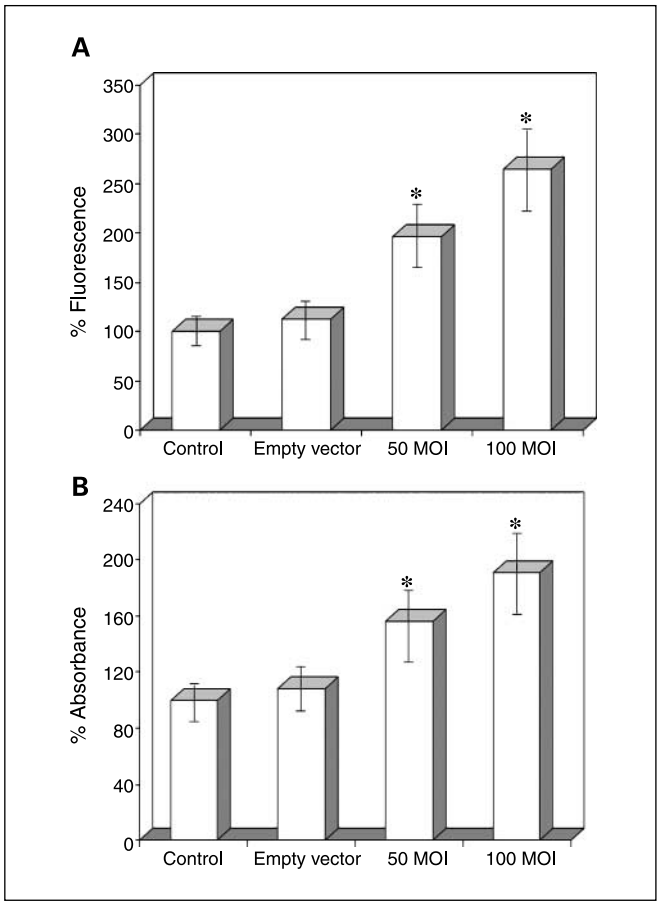

Fig. 4. *A,* caspase-9 fluorometric protease activity assay of rAAV-TFPI-2–transfected U-251 cells. Cells were transfected with 50 and 100 MOI of rAAV-TFPI-2. An empty vector transfected at a concentration of 100 MOI was used as a vector control. Data represent four independent experiments. *, $P < 0.001$. *B,* caspase-3 colorimetric protease activity assay of rAAV-TFPI-2–transfected U-251 cells. Cells were transfected with 50 and 100 MOI of rAAV-TFPI-2. An empty vector at a concentration of 100 MOI was used as a vector control. A standard curve was prepared with 100 μL of 10 to 200 μmol/L *p*-nitroaniline solution. Data are representative of four independent experiments. *, $P < 0.001$.

Caspase-3 is partially or totally responsible for the proteolytic cleavage of many key proteins, including the nuclear enzyme PARP and DFF45. In the current study, we observed a significant increase ($P < 0.001$) in caspase-3 activity after transfection of U-251 cells with rAAV-TFPI-2 at both 50 and 100 MOI (Fig. 4B). A 2-fold increase was observed in the activity of mature caspase-3 in U-251 cells transfected with rAAV-TFPI-2 at 100 MOI. Similar to the caspase-9 results, we detected no significant difference in caspase-3 activity between U-251 parental cells and cells transfected with the empty vector.

Double immunofluorescent staining reveals increased activity of caspase-9 and caspase-3. To confirm the increased activity of cleaved caspase-9 and cleaved caspase-3, we used double immunofluorescent staining and an electronic merging technique. We used cleaved caspase-9 and cleaved caspase-3 antibodies to avoid any cross-reaction with procaspase-9 and procaspase-3. The staining results clearly showed marked increases in the activity of both caspases after TFPI-2 restoration (Fig. 5B and C). In contrast, we detected no significant difference in the staining pattern between U-251 parental cells and the cells transfected with the empty vector; staining for both caspases was absent or insignificant. The double immunofluorescent staining for the active fragments of caspase-9 and caspase-3 illustrates the activity of both caspases in rAAV-TFPI-2–transfected cells. Further, nuclear counterstaining with Hoechst 33342 reveals several apoptotic cells after transfection with rAAV-TFPI-2 at both 50 and 100 MOI (Fig. 5A). The apoptotic cells were very prominent at concentrations of 50 and 100 MOI (Fig. 5D) after electronic merging of the Hoechst 33342 with caspase-9 and caspase-3 staining using Spot Advanced software.

TFPI-2 restoration increased the expression of death factors and death domains. Because TNF-α, FasL, and their respective death domains TRADD and FADD play key roles in apoptosis, we analyzed the protein levels of these important molecules after TFPI-2 restoration in U-251 cells. Apoptosis mediated by death factors, such as FasL and TNF-α, involves the formation of death-inducing signaling compound to their respective receptors (33). Western blot analysis revealed a significant increase in the protein levels of TNF-α, FasL, TRADD, and FADD after restoration of TFPI-2 in U-251 cells (Fig. 6A). There was no significant difference in the levels of all these molecules in the samples treated with the empty vector when compared with the parental cells. Reprobing and analysis of the nitrocellulose membrane for GAPDH clearly showed equal loading of protein in all the samples analyzed.

Increased mRNA expression of death factors and death domains. To study the expression of TNF-α, FasL, and related death domains at the transcriptional level, we analyzed the mRNA level of TNF-α, FasL, TRADD, and FADD using semiquantitative RT-PCR after TFPI-2 restoration. The results in Fig. 6B indicate significant increases in the mRNA levels of TNF-α, FasL, TRADD, and FADD after transfection of U-251 cells with rAAV-TFPI-2. In contrast, we detected no significant difference in the mRNA levels of any molecules studied cells transfected with the empty vector and parental cells. The increase in TNF-α mRNA was the most remarkable in comparison with the three other molecules measured. These results clearly indicate that TFPI-2 restoration plays a prominent role in the increased expression of TNF-α, FasL, and related death domains in U-251 cells. Again, GAPDH was used to ensure equal loading. Quantitative real-time RT-PCR analysis for the expression of TNF-α, FasL, TRADD, and FADD mRNA showed a similar pattern as of semiquantitative RT-PCR (Fig. 6C). The expression of all the genes screened was significantly elevated at 100 MOI with a maximum increase up to 330% for TRADD. At 50 MOI, the increase was significant only with TNF-α and TRADD.

Increased activity of caspases and executioners. In the present study, we observed increased levels of Bax and released cytochrome *c* (cytosolic fraction) after TFPI-2 restoration (Fig. 7A). Bcl-2, a major antiapoptotic molecule that inhibits mitochondrial cytochrome *c* release, was decreased significantly in TFPI-2–restored U-251 cells (Fig. 7A). We also observed significant increases in the expression of the cleaved fraction of lamin A, PARP, and the activated DNase (DFF40)—the three major apoptotic executioner molecules (Fig. 7B). Western blot analysis of major procaspases and cleaved caspase molecules involved in the apoptotic pathways is shown in Fig. 7C. The activities of all cleaved forms of caspase-10, caspase-9, caspase-8, caspase-7, caspase-6, and caspase-3 were increased after transfection of U-251 cells with rAAV-TFPI-2. The increased

levels of Bax, released cytochrome *c*, activated caspases, cleaved lamin, cleaved PARP, and DFF40 along with other results clearly indicate enhanced apoptosis after TFPI-2 restoration in U-251 glioblastoma cells. Stripping and reprobing of the nitrocellulose membrane for GAPDH indicated equal loading of proteins in all the samples analyzed.

Discussion

Apoptosis is the process of programmed cell death that occurs under numerous physiologic and pathologic conditions. It plays an important role in regulating cell growth, development, immune response, and the clearing of redundant or abnormal cells in organisms. The induction and execution of apoptosis require the coordination of a series of molecules, including signaling molecules, receptors, death domains, enzymes, and gene-regulating proteins. Resistance to apoptosis is a hallmark of cancer, and failure to execute apoptosis due to mutations of several genes provides cancer cells with an ability to survive and proliferate. Activation of apoptosis in cancer cells offers a novel and potentially useful approach to improve patient responses to conventional chemotherapy.

The imbalance between matrix-degrading proteases and their inhibitors, such as TFPI-2, plays a crucial role in tumor invasion and metastasis. The aberrant hypermethylation of TFPI-2 may be a common mechanism that contributes to the aggressive phenotype of brain tumor cells. It has been reported that the apoptosis of LSCC cells after restoration of *TFPI-2* gene may be connected with matrix metalloproteinase down-regulation (34). In addition to their role in ECM degradation, the proteinases also play an important role in regulating a wide variety of cellular functions, such as release of growth factors (35), which in turn promote the proliferation of the developing tumors. Thus, restoration TFPI-2 can inhibit tumor progression in a variety of ways through regulating the activity of proteinases, such as matrix metalloproteinases and plasmin. Furthermore, we have observed a total absence of matrix

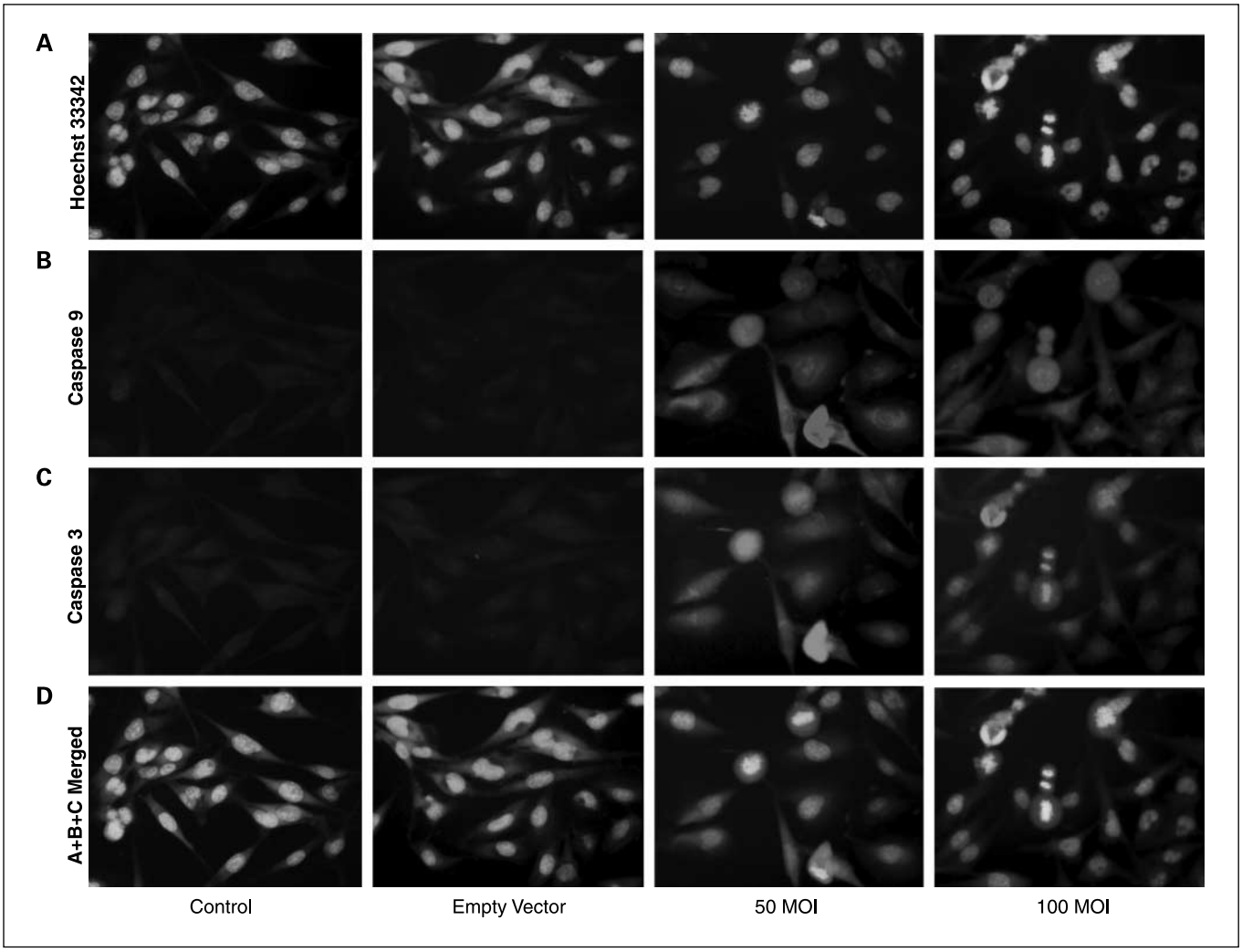

Fig. 5. Double immunofluorescent staining for caspase-9 and caspase-3 expression. U-251 parental cells were cultured on eight-well chamber slides at 2×10^3 per well and transfected with rAAV-TFPI-2 at concentrations of 50 and 100 MOI. An empty vector transfected at a concentration of 100 MOI was used as a vector control. Cells were blocked with 1% bovine serum albumin in PBS and incubated overnight at 4°C with mouse monoclonal caspase-9 and rabbit polyclonal caspase-3 primary antibodies simultaneously. Cells were washed and incubated with Texas red – conjugated anti-mouse and FITC-conjugated anti-rabbit secondary antibodies at room temperature for 1 h. The cells were then washed and treated with 1:100 diluted Hoechst 33342 for nuclear staining. *A,* Hoechst 33342. *B,* caspase-9. *C,* caspase-3. *D,* A+B+C merged.

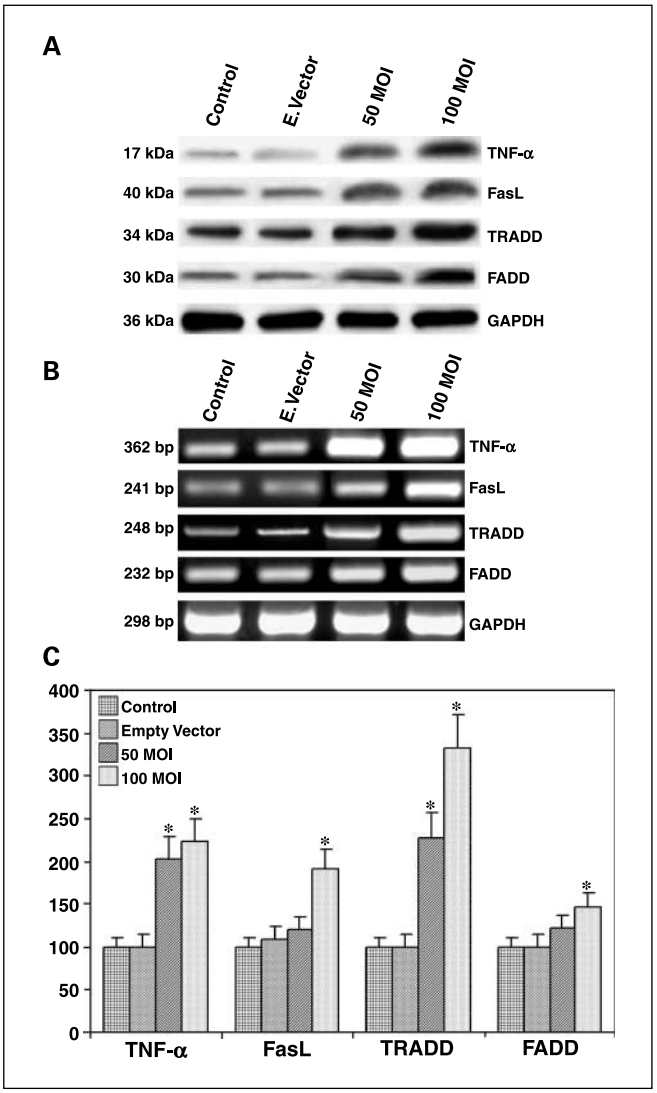

Fig. 6. *A,* Western blot analysis for the expression of TNF-α, FasL, FADD, and TRADD in rAAV-TFPI-2– transfected U-251 cells. Cells were transfected with 50 and 100 MOI of rAAV-TFPI-2. An empty vector (*E.Vector*) was transfected at a concentration of 100 MOI and used as a vector control. The membranes were reprobed for GAPDH content to show that similar amounts of protein were loaded in each lane. *B,* semiquantitative RT-PCR analysis for the expression of TNF-α, FasL, TRADD, and FADD mRNA in rAAV-TFPI-2– transfected U-251 cells using gene-specific primers. U-251 cells were transfected with rAAV-TFPI-2 at concentrations of 50 and 100 MOI. An empty vector transfected at a concentration of 100 MOI was used as a vector control. Total cellular RNA was isolated using RNeasy kit and ~100 μg were amplified on a PCR machine. *GAPDH* mRNA was used as a housekeeping gene. *C,* real-time RT-PCR analysis using SYBR Green and gene-specific primers for the quantitative evaluation of TNF-α, FasL, TRADD, and FADD mRNA expression. U-251 cells were transfected with rAAV-TFPI-2 at concentrations of 50 and 100 MOI. AAV-CMV transfected at a concentration of 100 MOI was used as an empty vector control. Columns, mean of six samples; bars, SD. *, $P < 0.001$.

metalloproteinase-9 activity in cultured Hs 683 cells, where TFPI-2 is highly expressed. These observations clearly indicate the significant role of TFPI-2 in the arrest of tumor cell invasion and metastasis.

In the present study, we successfully restored TFPI-2 protein in U-251 cells, in which the protein is totally absent due to lack of gene expression, through the use of highly efficient, replication-deficient adenoviral vectors expressing TFPI-2 cDNA. Various experiments, including the TUNEL assay for apoptosis and FACS analysis for DNA fragmentation, showed increased apoptosis after TFPI-2 restoration. Activity assay, double immunofluorescence, and Western blot analyses for various caspases showed increased expression of the cleaved active subunits of the caspases involved in the caspase cascade leading to apoptosis. Furthermore, Western blots and semiquantitative RT-PCR analyses showed increased expression of the death factors and death domains after restoration of TFPI-2 in U-251 cells. The study further depicted increased activity of apoptosis executioner molecules, such as cleaved PARP, cleaved lamin A, and DFF40. Our study is the first study with results that clearly show the mechanism of enhanced apoptosis in U-251 cells after restoration of TFPI-2 protein levels.

TNF-α is an important cytokine that plays a critical role in inflammatory responses and apoptosis (36). Other studies have reported that TNF-α is directly toxic to vascular endothelial cells that play a major role in angiogenesis during tumor invasion and metastasis (37). TNF-α induces apoptosis in cultured cerebral endothelial cells through the cleavage of caspase-3 (37). The function of TNF-α is mediated through two distinct cell surface receptors (TNFR1 and TNFR2). On ligand activation to the receptor, TNFR1 associates with death domain containing adaptor protein TRADD. TRADD, in turn, associates with FADD, which contains an NH_2-terminal death effector domain and binds to initiator caspase-8 (20). In the present study, we observed increased expression of both TNF-α and TRADD at both the mRNA and protein levels.

We have previously shown that restoration of TFPI-2 through adeno-associated viral vectors could prevent angiogenesis and tumorigenesis both *in vitro* and *in vivo* in SNB19 glioblastoma cells (13). Further, we observed the down-regulation of matrix metalloproteinase-9 and vascular endothelial growth factor as well as decreased angiogenesis and reduced cell invasion both *in vitro* and *in vivo* after restoration of TFPI-2 in U-251 cells.[4] These data suggest exertion of death stimulus after restoration of TFPI-2 through Bax, which in turn increases mitochondrial membrane permeability and leads to the release of cytochrome *c* from mitochondria. Bcl-2 exerts a survival function in response to apoptotic stimuli through inhibition of mitochondrial cytochrome *c* release (38). Here, we noted increased protein levels of Bax and released cytochrome *c*. These data suggest enhanced apoptotic stimuli after restoration of TFPI-2 in U-251 glioblastoma cells.

Caspases are interleukin-1β converting enzyme family proteases that initiate apoptosis in mammalian cells. Caspases are divided into initiator and effector (executioner) caspases depending on their site of action. Initiator caspases cleave inactive proforms of effector caspases, thereby activating them. Effector caspases, in turn, cleave other apoptotic executioner molecules, such as lamin A, DFF45, and PARP, resulting in cellular disassembly and DNA fragmentation. In the present study, we observed increased protein levels of cleaved (active) caspase-10, caspase-9, caspase-8, caspase-7, caspase-6, and caspase-3, which include both effector and executioner caspases after stable transfection of TFPI-2 in U-251 cells, where TFPI-2 protein is usually absent. Increased levels of executioner caspases, which are directly responsible for the cleavage of

[4] Unpublished data.

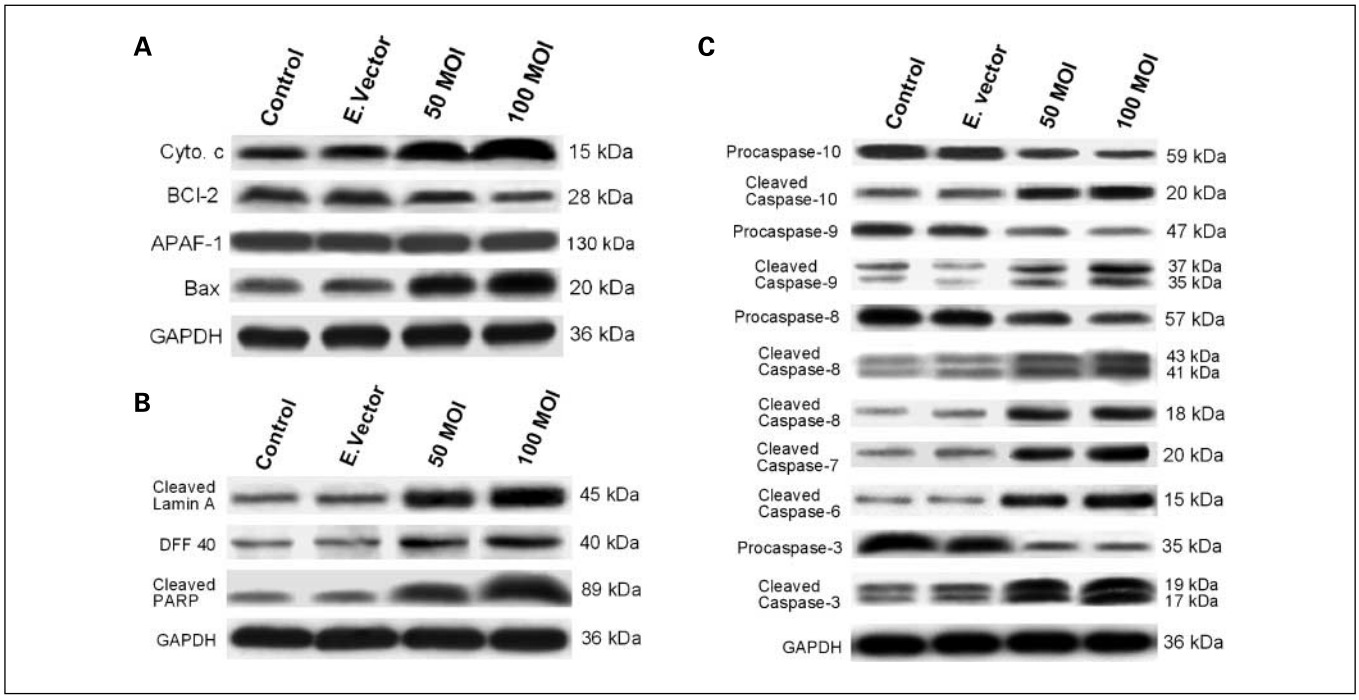

Fig. 7. *A,* Western blot analysis for cytochrome *c* (*Cyto. c*), Bcl-2, apoptotic protease-activating factor, and Bax in rAAV-TFPI-2–transfected U-251 cells. Cells were transfected with 50 and 100 MOI of rAAV-TFPI-2. An empty vector transfected at a concentration of 100 MOI was used as a vector control. Mitochondria were isolated from the total cell lysates, and the cytosol fraction was used to measure released cytochrome *c*. The nitrocellulose membranes were reprobed and analyzed for GAPDH content to show that similar amounts of protein were loaded in each lane. *B,* Western blot analysis for cleaved lamin A, DFF40, and cleaved PARP in rAAV-TFPI-2–transfected U-251 cells. Cells were transfected with 50 and 100 MOI of rAAV-TFPI-2. An empty vector transfected at a concentration of 100 MOI was used as a vector control. The nitrocellulose membranes were reprobed and analyzed for GAPDH content to show that similar amounts of protein were loaded in each lane. *C,* Western blot analysis for caspase-10, caspase-9, caspase-8, caspase-6, and caspase-3 in the cell lysates of rAAV-TFPI-2–transfected U-251 cells. Cells were transfected with 50 and 100 MOI of rAAV-TFPI-2. An empty vector transfected at a concentration of 100 MOI was used as a control. The nitrocellulose membranes were reprobed and analyzed for GAPDH content to show that similar amounts of protein were loaded in each lane.

apoptotic executioner molecules, clearly show enhanced apoptosis in U-251 cells after TFPI-2 restoration.

Lamins are intermediate filament proteins that form a matrix on the inner surface of the nuclear envelope. Lamin A is cleaved by caspase-6 and serves as a marker for caspase-6 activation. During apoptosis, the 70-kDa lamin A is specifically cleaved to a large 45-kDa fragment and a small 28-kDa fragment. Human DDF45 and its mouse homologue ICAD serve as chaperones for caspase-activated DNase during its synthesis (39). Caspase-3 is the primary enzyme responsible for processing DFF45 and release of its COOH-terminal fragment (40). On cleavage of DFF45/ICAD by activated caspase-3, DFF40/CAD is released and eventually causes DNA fragmentation, which is the hallmark of apoptotic cell death. Reports are not available about the role of TFPI-2 on either lamin A or DFF40/CAD. In the present study, we observed increased protein levels of both lamin A and DFF40, indicating enhanced nuclear disassembly and induction of apoptosis after TFPI-2 restoration.

PARP is a highly conserved nuclear enzyme present in higher eukaryotes. PARP is a DNA-binding protein that recognizes DNA strand breaks and is implicated in the DNA repair that occurs during apoptotic response. PARP cleavage has been shown to occur early in the apoptotic response as a result of caspase-3 activity (41). PARP cleavage correlates well with chromatin condensation, is associated with condensed chromatin in apoptotic cells, and precedes the ability to detect actual DNA fragmentation (42). Here, we observed a significant increase of cleaved PARP accompanied by chromatin condensation and DNA fragmentation—the hallmarks of apoptosis.

In conclusion, the results of the present study show that TFPI-2 restoration in a highly invasive glioblastoma cell line induces both intrinsic and extrinsic caspase-mediated pathway leading to apoptosis. Our study suggests that rAAV-mediated gene expression offers a novel and potential tool for cancer gene therapy.

Acknowledgments

We thank Shellee Abraham for secretarial assistance and Diana Meister and Sushma Jasti for reviewing the manuscript.

References

1. Pulkkanen KJ, Yla-Herttuala S. Gene therapy for malignant glioma: current clinical status. Mol Ther 2005; 12:585–98.
2. Donaldson SS, Laningham F, Fisher PG. Advances toward an understanding of brainstem gliomas. J Clin Oncol 2006;24:1266–72.
3. Combs SE, Widmer V, Thilmann C, Hof H, Debus J, Schulz-Ertner D. Stereotactic radiosurgery (SRS): treatment option for recurrent glioblastoma multiforme (GBM). Cancer 2005;104:2168–73.
4. Chand HS, Schmidt AE, Bajaj SP, Kisiel W. Structure-function analysis of the reactive site in the first

Kunitz-type domain of human tissue factor pathway inhibitor-2. J Biol Chem 2004;279:17500–7.

5. Rao CN, Peavey CL, Liu YY, Lapiere JC, Woodley DT. Partial characterization of matrix-associated serine protease inhibitors from human skin cells. J Invest Dermatol 1995;104:379–83.
6. Herman MP, Sukhova GK, Kisiel W, et al. Tissue factor pathway inhibitor-2 is a novel inhibitor of matrix metalloproteinases with implications for atherosclerosis. J Clin Invest 2001;107:1117–26.
7. Sugiyama T, Ishii S, Yamamoto J, et al. cDNA macroarray analysis of gene expression in synoviocytes stimulated with TNFα. FEBS Lett 2002;517:121–8.
8. Lino M, Foster DC, Kisiel W. Quantification and characterization of human endothelial cell-derived tissue factor pathway inhibitor-2. Arterioscler Thromb Vasc Biol 1998;18:40–6.
9. Rao CN, Reddy P, Liu Y, et al. Extracellular matrix-associated serine protease inhibitors (M_r 33,000, 31,000, and 27,000) are single-gene products with differential glycosylation: cDNA cloning of the 33-kDa inhibitor reveals its identity to tissue factor pathway inhibitor-2. Arch Biochem Biophys 1996; 335:82–92.
10. Petersen LC, Sprecher CA, Foster DC, Blumberg H, Hamamoto T, Kisiel W. Inhibitory properties of a novel human Kunitz-type protease inhibitor homologous to tissue factor pathway inhibitor. Biochemistry 1996;35: 266–72.
11. Chand HS, Du X, Ma D, et al. The effect of human tissue factor pathway inhibitor-2 on the growth and metastasis of fibrosarcoma tumors in athymic mice. Blood 2004;103:1069–77.
12. Konduri SD, Rao CN, Chandrasekar N, et al. A novel function of tissue factor pathway inhibitor-2 (TFPI-2) in human glioma invasion. Oncogene 2001;20:6938–45.
13. Yanamandra N, Kondraganti S, Gondi CS, et al. Recombinant adeno-associated virus (rAAV) expressing TFPI-2 inhibits invasion, angiogenesis and tumor growth in a human glioblastoma cell line. Int J Cancer 2005;115:998–1005.
14. Hajra KM, Liu JR. Apoptosome dysfunction in human cancer. Apoptosis 2004;9:691–704.
15. Strasser A, O'Connor L, Dixit VM. Apoptosis signaling. Annu Rev Biochem 2000;69:217–45.
16. Wajant H. CD95L/FasL and TRAIL in tumour surveillance and cancer therapy. Cancer Treat Res 2006;130: 141–65.
17. Chinnaiyan AM, O'Rourke K, Tewari M, Dixit VM. FADD, a novel death domain-containing protein, interacts with the death domain of Fas and initiates apoptosis. Cell 1995;81:505–12.
18. Nagata S, Golstein P. The Fas death factor. Science 1995;267:1449–56.
19. Ashkenazi A, Dixit VM. Death receptors: signaling and modulation. Science 1998;281:1305–8.
20. Hsu H, Shu HB, Pan MG, Goeddel DV. TRADD-TRAF2 and TRADD-FADD interactions define two distinct TNF receptor 1 signal transduction pathways. Cell 1996;84:299–308.
21. Hsu H, Xiong J, Goeddel DV. The TNF receptor 1-associated protein TRADD signals cell death and NF-κB activation. Cell 1995;81:495–504.
22. Liu X, Kim CN, Yang J, Jemmerson R, Wang X. Induction of apoptotic program in cell-free extracts: requirement for dATP and cytochrome *c*. Cell 1996; 86:147–57.
23. Susin SA, Zamzami N, Castedo M, et al. Bcl-2 inhibits the mitochondrial release of an apoptogenic protease. J Exp Med 1996;184:1331–41.
24. Zou H, Henzel WJ, Liu X, Lutschg A, Wang X. Apaf-1, a human protein homologous to *C. elegans* CED-4, participates in cytochrome *c*-dependent activation of caspase-3. Cell 1997;90:405–13.
25. Chandrasekar B, Vemula K, Surabhi RM, et al. Activation of intrinsic and extrinsic proapoptotic signaling pathways in interleukin-18-mediated human cardiac endothelial cell death. J Biol Chem 2004;279: 20221–33.
26. Li P, Nijhawan D, Budihardjo I, et al. Cytochrome *c* and dATP-dependent formation of Apaf-1/caspase-9 complex initiates an apoptotic protease cascade. Cell 1997;91:479–89.
27. Srinivasula SM, Fernandes-Alnemri T, Zangrilli J, et al. The Ced-3/interleukin 1β converting enzyme-like homolog Mch6 and the lamin-cleaving enzyme Mch2α are substrates for the apoptotic mediator CPP32. J Biol Chem 1996;271:27099–106.
28. Catchpoole DR, Lock RB. The potential tumour suppressor role for caspase-9 (CASP9) in the childhood malignancy, neuroblastoma. Eur J Cancer 2001;37: 2217–21.
29. Green DR, Kroemer G. The pathophysiology of mitochondrial cell death. Science 2004;305:626–9.
30. Joseph B, Marchetti P, Formstecher P, Kroemer G, Lewensohn R, Zhivotovsky B. Mitochondrial dysfunction is an essential step for killing of non-small cell lung carcinomas resistant to conventional treatment. Oncogene 2002;21:65–77.
31. Levkovitz Y, Gil-Ad I, Zeldich E, Dayag M, Weizman A. Differential induction of apoptosis by antidepressants in glioma and neuroblastoma cell lines: evidence for p-c-Jun, cytochrome *c*, and caspase-3 involvement. J Mol Neurosci 2005;27: 29–42.
32. Smith PK, Krohn RI, Hermanson GT, et al. Measurement of protein using bicinchoninic acid. Anal Biochem 1985;150:76–85.
33. Nagata S. Apoptosis by death factor. Cell 1997;88: 355–65.
34. Sun Y, Xie M, Liu M, Jin D, Li P. Growth suppression of human laryngeal squamous cell carcinoma by adenovirus-mediated tissue factor pathway inhibitor gene 2. Laryngoscope 2006;116:596–601.
35. McCawley LJ, Matrisian LM. Matrix metalloproteinases: they're not just for matrix anymore! Curr Opin Cell Biol 2001;13:534–40.
36. Aggarwal BB. Signalling pathways of the TNF superfamily: a double-edged sword. Nat Rev Immunol 2003;3:745–56.
37. Kimura H, Gules I, Meguro T, Zhang JH. Cytotoxicity of cytokines in cerebral microvascular endothelial cell. Brain Res 2003;990:148–56.
38. Murphy KM, Ranganathan V, Farnsworth ML, Kavallaris M, Lock RB. Bcl-2 inhibits Bax translocation from cytosol to mitochondria during drug-induced apoptosis of human tumor cells. Cell Death Differ 2000;7:102–11.
39. Enari M, Sakahira H, Yokoyama H, Okawa K, Iwamatsu A, Nagata S. A caspase-activated DNase that degrades DNA during apoptosis, and its inhibitor ICAD. Nature 1998;391:43–50.
40. Sakahira H, Enari M, Nagata S. Cleavage of CAD inhibitor in CAD activation and DNA degradation during apoptosis. Nature 1998;391:96–9.
41. Rosen A, Casciola-Rosen L. Macromolecular substrates for the ICE-like proteases during apoptosis. J Cell Biochem 1997;64:50–4.
42. Rosenthal DS, Ding R, Simbulan-Rosenthal CM, Vaillancourt JP, Nicholson DW, Smulson M. Intact cell evidence for the early synthesis, and subsequent late apopain-mediated suppression, of poly(ADP-ribose) during apoptosis. Exp Cell Res 1997;232: 313–21.